

Fabrication and characterization of the source grating for visibility improvement of neutron phase imaging with gratings

Jongyul Kim, Kye Hong Lee, Chang Hwy Lim, Taejoo Kim, Chi Won Ahn et al.

Citation: *Rev. Sci. Instrum.* **84**, 063705 (2013); doi: 10.1063/1.4810014

View online: <http://dx.doi.org/10.1063/1.4810014>

View Table of Contents: <http://rsi.aip.org/resource/1/RSINAK/v84/i6>

Published by the **AIP Publishing LLC**.

Additional information on *Rev. Sci. Instrum.*

Journal Homepage: <http://rsi.aip.org>

Journal Information: http://rsi.aip.org/about/about_the_journal

Top downloads: http://rsi.aip.org/features/most_downloaded

Information for Authors: <http://rsi.aip.org/authors>

ADVERTISEMENT

physicstoday

Comment on any
Physics Today article.

Physics Today / Volume 63 / Issue 7 / July 2012
Previous Article | Next Article

Measured energy in Japan

David von Seggern
(dvseg@seismo.unr.edu) University of Nevada
July 2012, page 10
DIGITAL OBJECT IDENTIFIER
<http://dx.doi.org/10.1063/PT.3.1619>

The article by Thorne Lay and Hiroo Kanamori (10.1063/PT.3.1619) is an excellent review of the energy released by the 2011 Tohoku earthquake and tsunami. It is an excellent example of the relationship between seismic moment and energy release. The authors state that the energy released by the earthquake was approximately five times as much energy as that of a 100-megaton atmospheric nuclear detonation event—a 10-megaton nuclear device had still more energy by a factor of about 3, or 15 times that of a 100-megaton atmospheric nuclear detonation event.

The 1964 Chilean earthquake had still more energy by a factor of about 3, or 15 times that of a 100-megaton atmospheric nuclear device. I believe the authors used the relation for seismic energy release rather than total strain energy release. The seismic energy underestimates the total strain energy release by a variable that depends on friction on the fault plane. Accounting for total strain energy release would increase the earthquake energy number by orders of magnitude.

Despite the catastrophic damage potential of nuclear bombs, the forces of nature occasionally unleash much larger energy releases. Although the nuclear bombs are under our control, earthquakes, volcanic eruptions, and extreme weather events are not. However, by judicious preparation and avoidance measures, humans can significantly diminish the damage of natural events.

This article does not have any references.

Comment on this article

By the act of hitting a ball with a bat, one calculates the force energy to deliver the ball to its new location, but one must also take into account that the ball extended its energy to the strike team, which became struck by the ball as its momentum ceased and passed energy to the strike team. Therefore the parameters of the damage extend into the future when the received energy to that pushed upon, later becomes released in a new event. Perhaps calculations of one added that in, while another's calculations did not. E.M.C.

Written by Edgar McCarroll, 14 July 2012 19:59

Fabrication and characterization of the source grating for visibility improvement of neutron phase imaging with gratings

Jongyul Kim,^{1,2} Kye Hong Lee,¹ Chang Hwly Lim,¹ Taejoo Kim,¹ Chi Won Ahn,³ Gyuseong Cho,² and Seung Wook Lee^{4,a)}

¹Neutron Science Division, Korea Atomic Energy Research Institute, Daejeon 305-353, South Korea

²Nuclear and Quantum Engineering Department, Korea Advanced Institute of Science and Technology, Daejeon 305-701, South Korea

³Nano Fusion Technology Division, National Nanofab Center, Daejeon 305-701, South Korea

⁴School of Mechanical Engineering, Pusan National University, Pusan 609-735, South Korea

(Received 10 April 2013; accepted 27 May 2013; published online 27 June 2013)

The fabrication of gratings including metal deposition processes for highly neutron absorbing lines is a critical issue to achieve a good visibility of the grating-based phase imaging system. The source grating for a neutron Talbot-Lau interferometer is an array of Gadolinium (Gd) structures that are generally made by sputtering, photo-lithography, and chemical wet etching. However, it is very challenging to fabricate a Gd structure with sufficient neutron attenuation of approximately more than 20 μm using a conventional metal deposition method because of the slow Gd deposition rate, film stress, high material cost, and so on. In this article, we fabricated the source gratings for neutron Talbot-Lau interferometers by filling the silicon structure with Gadox particles. The new fabrication method allowed us a very stable and efficient way to achieve a much higher Gadox filled structure than a Gd film structure, and is even more suitable for thermal polychromatic neutrons, which are more difficult to stop than cold neutrons. The newly fabricated source gratings were tested at the polychromatic thermal neutron grating interferometer system of HANARO at the Korea Atomic Energy Research Institute, and the visibilities and images from the neutron phase imaging system with the new source gratings were compared with those fabricated by a Gd deposition method. © 2013 AIP Publishing LLC. [<http://dx.doi.org/10.1063/1.4810014>]

I. INTRODUCTION

Neutron and X-ray differential phase contrast and dark-field imaging methods based on Talbot-Lau interferometer have been developed over the last few years.^{1–8} Neutron dark-field imaging has been demonstrated to be able to visualize the magnetic domains of magnetic materials owing to a strong dark-field signal from magnetic domain walls, and the three-dimensional image of magnetic domain structures within the bulk of FeSi crystals can be obtained using neutron dark-field tomography.^{9,10} Although neutron dark-field imaging shows a great potential for the investigation of internal magnetic domain structures, improved image quality is demanded for more detailed information. A Talbot-Lau neutron interferometer consists of three diffraction gratings: a source grating G0, a phase grating G1, and an analyzer grating G2, as illustrated in Fig. 1. The source grating G0 transforms large incoherent neutron sources into line sources, which provide enough spatial coherence for the interference pattern, and the phase grating G1 as a beam splitter creates the interference patterns at Talbot distances. Since the neutron imaging detector cannot resolve the interference pattern directly, the analyzer grating G2 is used for phase stepping scan method.^{11–13} After the phase stepping scan, the visibilities of the interferometer can be evaluated using the intensity modulation of each detector pixel. The intensity modulation and visibility in each detector

pixel can be expressed by

$$I(m, n, x_g) = \sum_k a_k(m, n) \cos \left[k \frac{2\pi}{p_2} x_g + \varphi_k(m, n) \right], \quad (1)$$

$$V(m, n) = \frac{a_1(m, n)}{a_0(m, n)}. \quad (2)$$

The visibility can be degraded by many factors, an important one of which is the quality of the gratings,¹⁴ and the decreased visibility affects the image quality of both the differential phase contrast and dark-field imaging. The fabrication process of phase grating with silicon structures is well established. However, the fabrication of gadolinium (Gd) structures for source and analyzer gratings is quite annoying due to the use of uncommon materials for deposition and etching, and thus the development of different fabrication processes is needed. The conventional source grating G0 is fabricated using sputtering and a chemical wet etching process. For neutron wavelength $\lambda = 4.4 \text{ \AA}$, the Gd structure height should be more than 10 μm for a sufficient neutron absorption of more than 97%. A Gd deposition of 10 μm is quite difficult because of the residual stress in the deposited film, which depends on film thickness, deposition rate, substrate temperature, and so on. A thicker deposited film tends to result in a higher residual stress.^{15,16} In addition, the grating walls are not vertical because the wet etching process for the Gd structure is isotropic. The fabrication of analyzer grating G2 using an evaporation process is more complicated. In this article, we propose new fabrication method for a source grating

^{a)}Electronic mail: seunglee@pusan.ac.kr

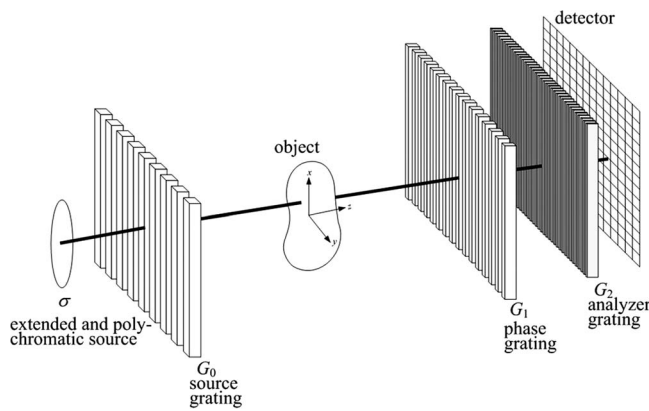


FIG. 1. Schematic of a neutron grating interferometer.

that has the Gd structure of enough height to improve the visibility. The source grating fabricated by the new method is able to work with a thermal polychromatic spectrum since the new source grating is designed to absorb the thermal neutrons around $\lambda = 2.0 \text{ \AA}$ sufficiently. The performance of the new source grating was tested at the Ex-core Neutron irradiation Facility (ENF) of HANARO at the Korea Atomic Energy Research Institute (KAERI) by evaluating the visibility.

II. FABRICATION OF NOVEL SOURCE GRATING

The source grating G_0 was newly fabricated using a Gadolinium Oxysulfide (Gadox) filling method instead of a Gd deposition method. The new source grating G_0 for $\lambda = 4.4 \text{ \AA}$ is designed to have a period of $774 \mu\text{m}$, a duty cycle of 0.4, and a Gd structure height of $500 \mu\text{m}$ to absorb neutrons sufficiently when a lower packing density of the Gd structure by a Gadox filling method is considered. The following steps shown in Fig. 2 are used to fabricate the new source grating. The first step is the fabrication of silicon structures,

which was performed at the National Nanofab Center (NNFC) at the Korea Advanced Institute of Science and Technology (KAIST). A 15 cm silicon wafer with a thickness of $700 \mu\text{m}$ is used, and negative photoresist material is spin-coated onto a silicon wafer. After the spin-coating process, a standard photolithography process is used for photoresist patterning. The silicon wafer is then etched using a deep reactive ion etching (DRIE) process. The width of the etched area is $477 \mu\text{m}$ for a duty cycle of 0.4, and the height of silicon structure is $500 \mu\text{m}$. An optical microscopy image of the fabricated silicon grating surface is shown in Fig. 4(a). The second step is the filling of Gadox particles into the fabricated silicon structures. Gadox has been widely used as a neutron scintillation material for high resolution neutron imaging due to a high cross section for thermal neutron absorption when compared with other materials. To bind Gadox particles with an average size of $5 \mu\text{m}$, a binding solution composed of texanol and acrylic resin with a mass ratio of 8:1 is used. Gadox particles and the binding solution are mixed with a mass ratio of 4:1 in a conditioning mixer, ARE-250. The Gadox mixture is then poured onto the fabricated silicon structures. After precipitation of the Gadox particles, the remaining Gadox mixture on the silicon structures is removed, and texanol is evaporated to solidify in an oven at 150°C for 10 min. The source grating fabricated by the Gadox filling method is shown in Fig. 3. From the scanning electron microscopy (SEM) images, we confirmed that the fabricated silicon grating is successfully filled with Gadox particles. The SEM images of the new source grating are shown in Figs. 4(b) and 4(c). The neutron projection images of the source gratings were obtained using a conventional radiography system at ENF, which has a polychromatic neutron source to compare the neutron transmittance of the newly fabricated source grating with that of a conventional source grating and are shown in Figs. 5(a)–5(c). In Fig. 5(d), the line profile of the projection images shows that the new source grating more sufficiently absorbs the thermal neutrons than the conventional source grating.

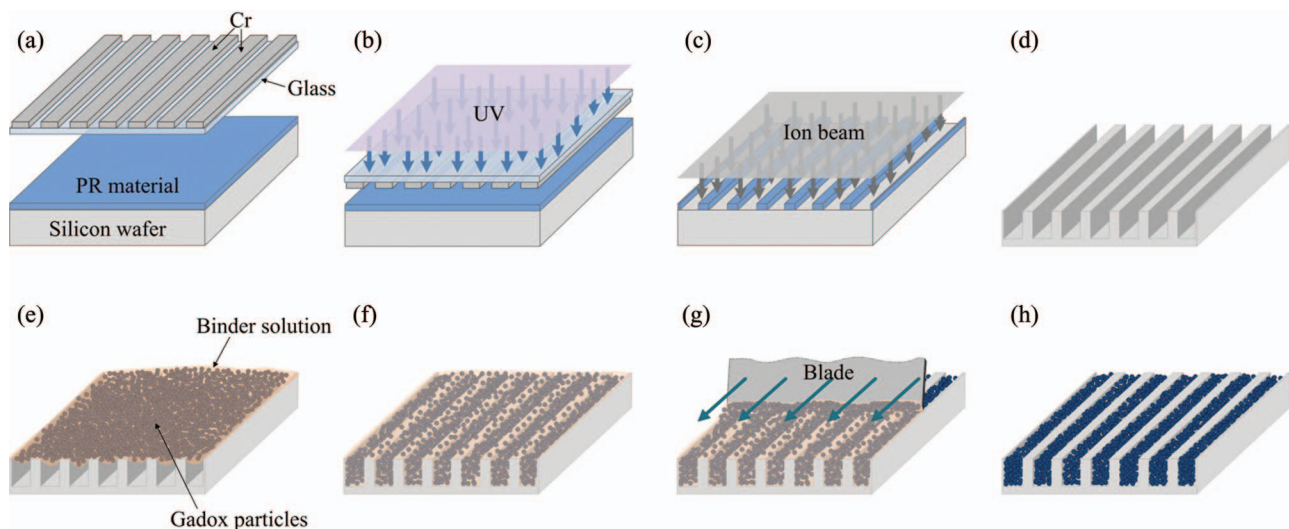


FIG. 2. Fabrication process of new source grating: (a) photoresist material coating, (b) UV exposure and development, (c) deep reactive ion etching, (d) fabricated silicon structure, (e) pouring Gadox mixture, (f) precipitation of Gadox particles in vacuum chamber, (g) removing of remained Gadox particles, and (h) solidification in an oven.

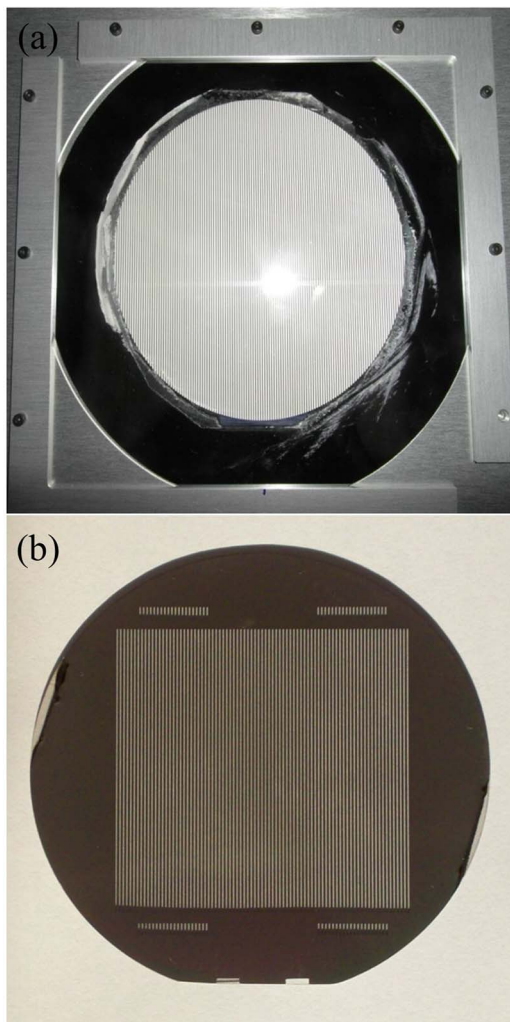


FIG. 3. (a) A source grating fabricated by the Gadox filling method and (b) a source grating fabricated by the Gd deposition method.

III. CHARACTERIZATION OF SOURCE GRATINGS

The neutron grating interferometer setup was established at ENF, as shown in Fig. 6, and the parameters of the grating interferometer setup are given in Table I. The newly fabricated and conventional source gratings were tested with a polychromatic and quasi-monochromatic spectrum. Beryllium filters with 5 cm and 10 cm thicknesses were used for the spectral shaping by cutting off below 4 Å. The mean wavelengths

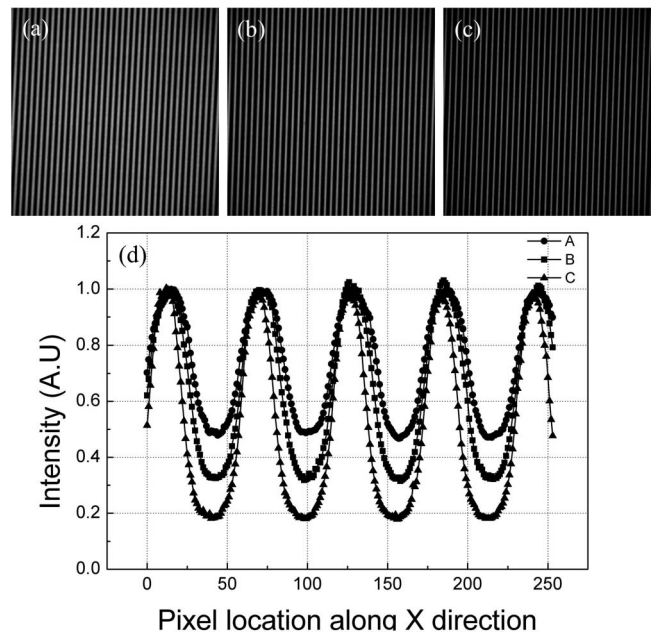


FIG. 5. The neutron transmission images: (a) a conventional source grating with a 5 μm height, (b) a conventional source grating with a 10 μm height, (c) the new source grating, and (d) a line profile of the projection images.

of the polychromatic and quasi-monochromatic spectrum are 2.7 Å and 4.4 Å, respectively. To obtain and evaluate their visibilities, the measured pixel values by phase stepping and sine fitting curve as shown in Fig. 7 are used, and amplitude coefficients a_1 and a_0 are obtained from the sine fitting curve. The measured pixel values with and without Beryllium are obtained from 10 images with 120 s and 60 s exposure times. The visibilities of the neutron grating interferometer setup including new and conventional source gratings in accordance with the Beryllium filter thickness are shown in Table II. To find the accurate Talbot distance, visibilities were scanned at a different G1-G2 distance around the calculated first Talbot distance, and the measured visibilities are shown in Fig. 8. The G1-G2 distance of maximum visibility at each test condition was about 1.82 cm.

IV. RESULTS

When comparing the visibilities of the neutron grating interferometer setup including new and conventional source

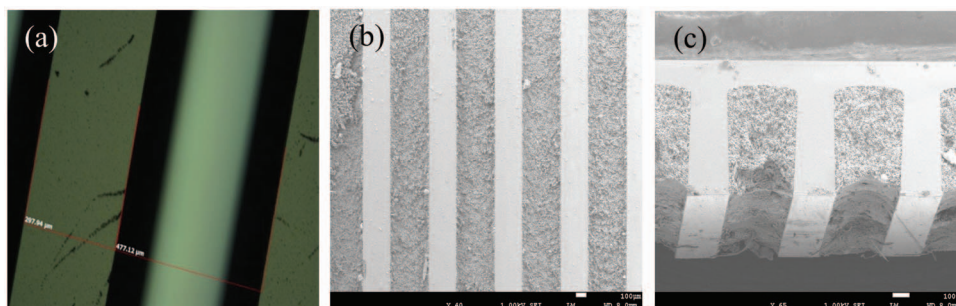


FIG. 4. (a) An optical microscopy image of the fabricated silicon grating surface, (b) SEM images of the grating surface, and (c) SEM images of the grating cross section.

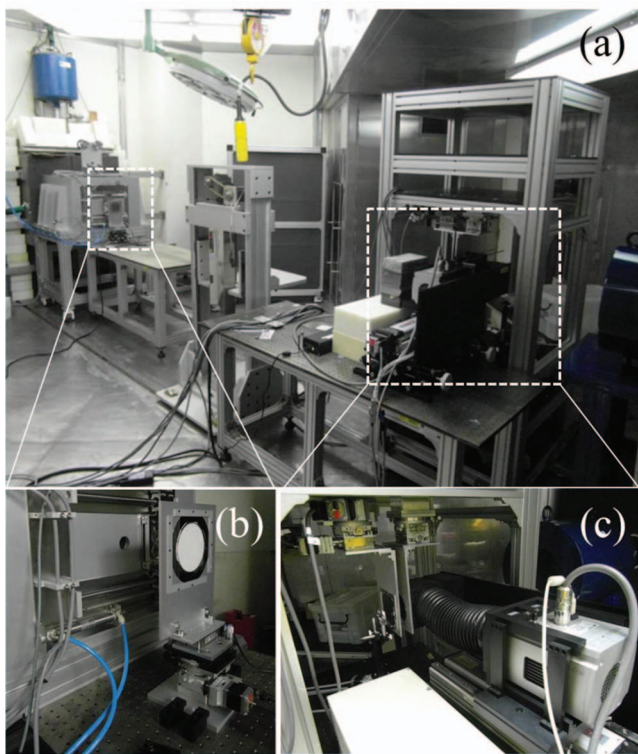


FIG. 6. Neutron grating interferometer setup at ENF: (a) overview of the inside ENF, (b) the source grating G0 and motorized stage, and (c) the phase grating G1, the analyzer grating G2, the lens coupled detector with a scintillation screen, and the motorized stage.

TABLE I. Parameters of the designed grating interferometer setup at ENF.

Geometrical and grating parameters	
Designed wavelength	4.4 Å
G0-G1 distance	350 cm
G1-G2 distance, First Talbot distance	1.82 cm
Phase grating G1 (π -shifting)	Silicon, $p_1 = 7.96 \mu\text{m}$, $h_1 = 34.39 \mu\text{m}$
Analyzer grating G2	Gd, $p_2 = 4 \mu\text{m}$, $h_2 = 3 \mu\text{m}$
New source grating G0	Gadox, $p_0 = 774 \mu\text{m}$, $h_0 = 500 \mu\text{m}$
Conventional source grating G0	Gd, $p_0 = 774 \mu\text{m}$, $h_0 = 10 \mu\text{m}$

TABLE II. G0 grating test conditions and visibilities.

Test no.	Fabrication method	Gd structure height (μm)	Beryllium filter (cm)	Visibility at the first Talbot distance (%)
1	Gd deposition	10	0	3.7
2	Gd deposition	10	5	11.5
3	Gadox filling	500	0	6.4
4	Gadox filling	500	5	15
5	Gadox filling	500	10	18

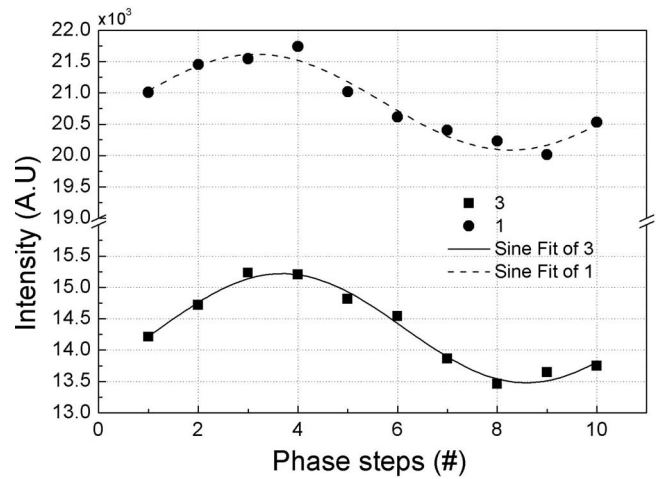


FIG. 7. Measured pixel values by phase stepping and sine fitting curve.

gratings without a Beryllium filter, the visibilities of the new and conventional setup are 6.4% and 3.7%, respectively. The reason for the higher visibility of the new setup is that the thermal neutrons below 4 Å of the polychromatic beam are more efficiently absorbed with the new source grating. The average A0 values of the new and conventional setup without a Beryllium filter are 14 000 and 21 200, respectively. The average A1 values of the new and conventional setup without a Beryllium filter are 835 and 793, respectively. The higher visibility could be obtained using the new source grating without a Beryllium filter because of a reduction of the average A0. In the experiment on the new and conventional setups with a 5 cm Beryllium filter, the visibilities are 15% and 11.5%, respectively. The visibility of the new setup is still higher than the conventional one. Although the neutrons below 4 Å are decreased by Beryllium filters with 5 cm, there are some neutrons below 4 Å. The 18% visibility of the new setup with a 10 cm Beryllium filter is achieved. The neutron dark-field images with the new source grating of the FeSi sample are shown in Fig. 9, and the increased visibility improves the image quality when compared with the dark-field images with a 5 cm and 10 cm Beryllium filter. However, the data acquisition time increases as a thicker Beryllium filter is used because of the flux reduction by a Beryllium filter and the neutron flux data can be found in Ref. 5. The average A0 values of the new setup were, respectively, 28 106, 2104, and 921 in accordance with Beryllium filter thicknesses of 0 cm, 5 cm, and 10 cm at 120 s exposure time.

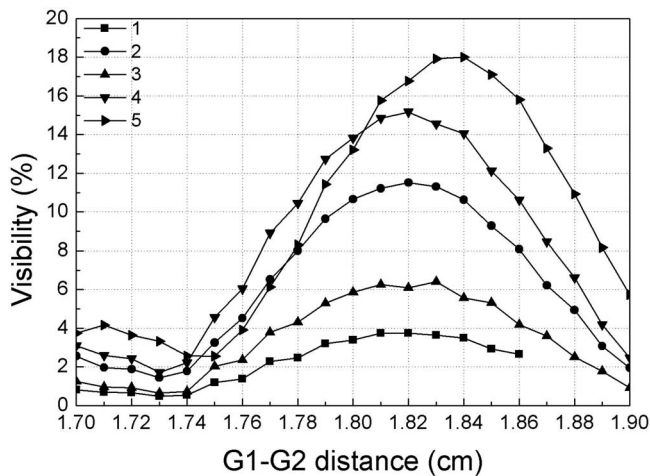


FIG. 8. The optimization of visibility by changing the G1-G2 distance.

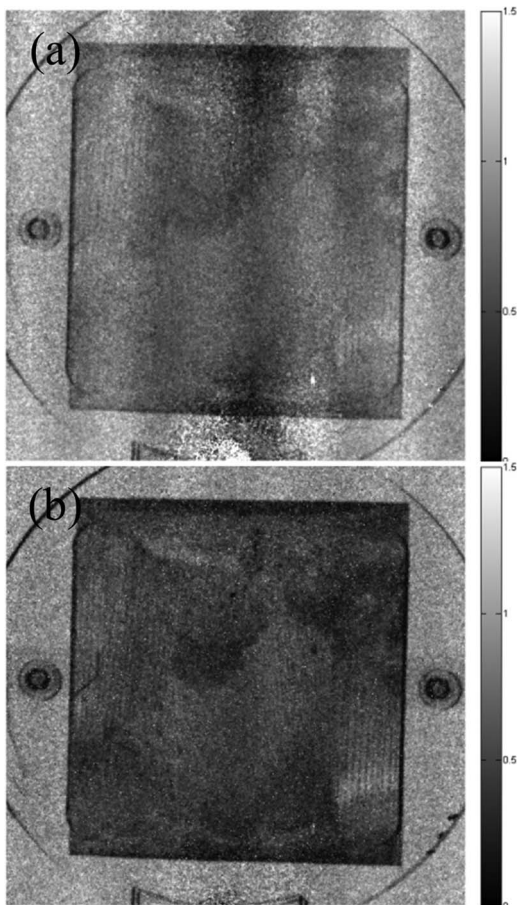


FIG. 9. (a) A dark-field image with the new source grating and a 5 cm Beryllium filter of the FeSi sample, and (b) a dark-field image with the new source grating and a 10 cm Beryllium filter of the FeSi sample.

V. CONCLUSION

A new source grating was successfully fabricated by a Gadox filling method, and the neutron grating interferometer setup including a new source grating works with a polychromatic spectrum at ENF. In addition, the visibility of the setup increases when the new source grating is used. A Gd deposition of $10\ \mu\text{m}$ is quite difficult because Gd is an uncommon material for a deposition method. On the other hand, the fabrication of the source grating by Gadox filling method is fairly easy since a silicon etching process is used. In addition, the source grating pitch of the neutron grating interferometer is wide enough to fill the Gadox particles sufficiently. Using the Gadox filling method, source gratings for other wavelengths such as $2\ \text{\AA}$, $2.7\ \text{\AA}$, and $3.5\ \text{\AA}$ can be fabricated since the new source grating is designed to absorb thermal neutrons sufficiently. A neutron grating interferometer with a polychromatic spectrum could shorten the data acquisition time because of a higher neutron flux. In further work, new source gratings for other wavelengths will be fabricated and tested with a polychromatic spectrum to shorten the data acquisition time and find the optimized visibility. The fabrication of analyzer gratings may also be tried with the Gadox filling method.

ACKNOWLEDGMENTS

This work was supported by the Nuclear Research and Development Program of the National Research Foundation of Korea (NRF) grant funded by the Korean Ministry of Science, ICT and Future Planning (MSIP).

- ¹F. Pfeiffer, C. Grünzweig, O. Bunk, G. Frei, E. Lehmann, and C. David, *Phys. Rev. Lett.* **96**, 215505 (2006).
- ²C. Grünzweig, F. Pfeiffer, O. Bunk, T. Donath, G. Kühne, G. Frei, M. Dierolf, and C. David, *Rev. Sci. Instrum.* **79**, 053703 (2008).
- ³M. Strobl, C. Grünzweig, A. Hilger, I. Manke, N. Kardjilov, C. David, and F. Pfeiffer, *Phys. Rev. Lett.* **101**, 123902 (2008).
- ⁴S. W. Lee, H. S. Hussey, D. S. Jacobson, C. M. Sim, and D. Arif, *Nucl. Instrum. Methods Phys. Res. A* **605**, 16 (2009).
- ⁵S. W. Lee, Y. K. Jun, and O. Y. Kwon, *J. Korean Phys. Soc.* **58**, 730 (2011).
- ⁶C. Kottler, F. Pfeiffer, O. Bunk, C. Grünzweig, and C. David, *Rev. Sci. Instrum.* **78**, 043710 (2007).
- ⁷T. Donath, F. Pfeiffer, O. Bunk, W. Groot, and M. Bednarzik, *Rev. Sci. Instrum.* **80**, 053701 (2009).
- ⁸J. Herzen, T. Donath, F. Beckmann, M. Ogurreck, and C. David, *Rev. Sci. Instrum.* **82**, 113711 (2011).
- ⁹S. W. Lee, K. Y. Kim, O. Y. Kwon, N. Kardjilov, M. Dawson, A. Hilger, and I. Manke, *Appl. Phys. Express* **3**, 106602 (2010).
- ¹⁰I. Manke, N. Kardjilov, R. Schäfer, A. Hilger, M. Strobl, M. Dawson, C. Grünzweig, G. Behr, M. Hentschel, C. David, A. Kupsch, A. Lange, and J. Banhart, *Nat. Commun.* **1**, 125 (2010).
- ¹¹A. Momose, *Opt. Express* **11**, 2303 (2003).
- ¹²T. Weitkamp, A. Diaz, C. David, F. Pfeiffer, M. Stampanoni, P. Cloetens, and E. Ziegler, *Opt. Express* **13**, 6296 (2005).
- ¹³F. Pfeiffer, T. Weitkamp, O. Bunk, and C. David, *Nat. Phys.* **2**, 258 (2006).
- ¹⁴M. Chabior, M. Schuster, M. Goldammer, C. Schroer, and F. Pfeiffer, *Nucl. Instrum. Methods Phys. Res. A* **683**, 71 (2012).
- ¹⁵J. A. Thornton and D. W. Hoffman, *Thin Solid Films* **171**, 5 (1989).
- ¹⁶C. W. Tan and J. Miao, *Thin Solid Films* **517**, 4921 (2009).